Laser Physics Letters

Astro Ltd.

LETTER

Stable high-efficiency continuous-wave diamond Raman laser at 1178 nm

To cite this article: Yuxiang Sun *et al* 2022 *Laser Phys. Lett.* **19** 125001

IOP Publishing | Astro Ltd Laser Physics Letters
Laser Phys. Lett. **19** (2022) 125001 (6pp) https://doi.org/10.1088/1612-202X/ac9ce2

Letter

Stable high-efficiency continuous-wave diamond Raman laser at 1178 nm

Yuxiang Sun[1,2], Muye Li[2], Ondrej Kitzler[3], Richard Paul Mildren[3], Zhenxu Bai[4], Hongchao Zhang[1], Jian Lu[1], Yan Feng[2,5] and Xuezong Yang[2,*]

[1] School of Science, Nanjing University of Science & Technology, Nanjing 210094, People's Republic of China
[2] Department of Physics and Optoelectronic Engineering, Hangzhou Institute for Advanced Study, University of Chinese Academy of Sciences, Hangzhou 310024, People's Republic of China
[3] MQ Photonics Research Centre, Department of Physics and Astronomy, Macquarie University, Sydney, NSW 2109, Australia
[4] Center of Advanced Laser Technology, Hebei University of Technology, Tianjin 300401, People's Republic of China
[5] Shanghai Institute of Optics and Fine Mechanics, Chinese Academy of Sciences, Shanghai 201800, People's Republic of China

E-mail: xuezong.yang@ucas.ac.cn

Received 16 August 2022
Accepted for publication 13 October 2022
Published 2 November 2022

Abstract

We demonstrate a high-efficiency continuous-wave (CW) diamond Raman laser operating at 1178 nm with enhanced stability by using a V-cavity design. A maximum Stokes power of 39 W with a conversion efficiency of 45% was achieved using a linearly-polarized 1018 nm Yb-doped fiber pump laser. The Stokes CW power stability showed superior stability over a linear cavity when characterized over periods up to 15 min. The Stokes output was found to switch between linear, elliptical, and random polarization with varying pump polarization. The results represent a major step towards stable, efficient and high-power CW lasers at 1178 nm and at wavelengths outside the main Yb, and Nd emission bands.

Keywords: diamond Raman laser, stimulated Raman scattering, stable high-efficiency resonator, optical frequency conversion

(Some figures may appear in colour only in the online journal)

1. Introduction

Sodium guide star lasers at 589 nm are widely used in ground optical telescopes for the applications in astronomical observations, mesospheric sensing, ground-space communication and space debris tracking [1–8]. Frequency doubling of 1178 nm lasers [9–11, 12] and frequency mixing of two lasers with separate wavelengths [13–15] are two common technologies to access this interesting wavelength. Owing to its versatile output wavelength, self-phase-matching physical condition and extreme conversion efficiency, stimulated Raman scattering (SRS) laser has been well established as a means of producing the lasing wavelength at 1178 nm [11, 16, 17–22]. Raman fiber laser technology [10, 21] stands out among all current possible 1178 nm laser technologies due to its high output power, high beam quality and robustness. However, the Raman frequency shift in fiber is small (495 cm^{-1}) so complex laser design is required to achieve longer wavelength output (such as 1178 nm corresponding to the second-order Raman conversion with a

* Author to whom any correspondence should be addressed.

normally used 1064 nm pump laser). Besides, it is relatively difficult for Raman fiber oscillator to obtain a high-power narrow linewidth (tens of GHz) Stokes laser [23]. In parallel, a wide variety of crystalline Raman lasers, such as $BaWO_4$, $CaWO_4$, and Nd:YVO_4 [18–20, 22, 24], have been investigated to deliver the wavelength described above, however, the output powers are restricted to watt-level due to their limited heat handling capacity.

Single-crystal diamond has drawn great attention for the last decade in the application of Raman lasers and been considered as a promising technology to produce Raman lasing with better performance [25–28]. Diamond has outstanding advantages in the high-power regime [26, 29, 30] by virtue of its extremely outstanding thermophysical and SRS properties [31], high thermal conductivity (2200 $W\,m^{-1}\,K^{-1}$), low linear thermal expansion coefficient ($1.1 \times 10^{-6}\,K^{-1}$), wide optical transmission spectrum from 225 nm to mid IR, high Raman gain coefficient from 8 to 10 $cm\,GW^{-1}$ at 1064 nm, large Raman frequency shift of 1332.3 cm^{-1}. Recently, several reports have shown that Raman lasing in diamond is an interesting method for developing 1178 nm laser based on mature Yb-doped fiber (YDF) lasers at 1018 nm as pumps [32–34]. In [32], a diamond Raman laser (DRL) converted a continuous pumping power of 250 W at 1018 nm to the first-order Stokes wave at 1178 nm with the output power of 46 W having a conversion efficiency of 23% and a slope efficiency of 25%. Here the overall efficiency was relatively low, due to the single-pass of the pump through the diamond, and because of the lower gain provided in the case of a circular pump polarization and broad linewidth. In [33], 0.7 W output at 1178 nm was obtained using an intracavity second-harmonic laser alongside 22 W of output at 589 nm. And in [34], 35 W Stokes laser at 1178 nm was reported at 32% conversion efficiency. It is worth noting that all the works to date [25, 27, 32, 33, 35] have only used linear cavity structure and have no detailed study about the long-term stability of the Stokes output. As we know, for narrow-bandwidth pump lasers, these pump double-passed linear cavities are very sensitive to intracavity pump resonance which will aggravate the Stokes instability.

In this paper, a continuous-wave (CW) DRL at 1178 nm is investigated for a V-shaped Raman cavity operating with pump powers up to 86 W. The amplitude stability is compared for a linear cavity using the same pump laser. Although some stimulated Brillouin scattering (SBS) is generated by the intracavity Raman field, intense temporal fluctuations are not observed, and stable output power up to 39 W is obtained with a root mean square (RMS) less than 2.4%.

2. Experimental setup

The schematic configuration is shown in figure 1. A homemade CW YDF laser at 1018 nm with linear polarization and narrow linewidth to enhance the gain and reduce the Raman threshold [26, 36–38]. The pump offered a maximum output power of 90 W, power stability RMS within 1%, full width at half maximum (FWHM) linewidth of 12 GHz, beam quality of $M^2 = 1.45$ and polarization extinction ratio (PER) of 25 dB. A thermal lens compensated isolator (SteadiBeam, AFR Ltd) is placed after the pump to protect it against the backward beam propagation. As illustrated in the blue dashed box in figure 1, the Raman laser cavity was a V-shaped cavity composed of two concave mirrors and a planar mirror (M1). The IC and OC had the same radius of curvature (Roc) of 50 mm. The separation distances from IC to OC and from IC to M1 were 81 mm and 150 mm, respectively. Thus the Raman resonator had a propagation length of 231 mm and its fundamental transverse-mode waist radius was 28 μm. The IC and M1 had the same optical coatings of highly transmissive (94.5%T) at 1018 nm and highly reflective (>99.9%R) at 1178 nm. The coating of OC had about 1% transmittance at 1178 nm and was highly reflective (99.8%R) at 1018 nm, which enabled a pump double pass architecture. The diamond Raman crystal (type IIa CVD-grown) had dimensions of $7 \times 4 \times 1.2\,mm^3$ and its end facets were antireflection coated at both 1018 nm and 1178 nm. The diamond crystal was inserted at the waist of the resonator and mounted in a water-cooled aluminum holder maintained at 22 °C. A plano-convex lens (L1) with a focal length of $f = 75$ mm was used to focus the pump tightly in the diamond, providing a pump spot radius of 24 μm. The polarization of the pump was aligned along the [111] axis of the diamond crystal by a half-wave plate (HWP) to attain the highest gain. For a comparative investigation of the stability of the V-shaped cavity, an external linear diamond Raman cavity was concurrently constructed, whose scheme resembled that reported in [39]. Although an OC with Roc of 75 mm was adapted in the linear cavity, the coatings of both IC and OC were the same as those in the V-shaped cavity to provide highly consistent experimental conditions.

3. Results and discussion

The measured power of Stokes and residual pump for the V-cavity was shown in figure 2. The Stokes lasing threshold was 21 W. Above the threshold, the Stokes output power increased proportionally with increasing pump power and its slope efficiency was up to 58.6%. The maximum output power was 39 W obtained with 86 W pump power, which corresponded to a conversion efficiency of 45%. The residual pump power, measured at the isolator as shown in figure 1 was strongly depleted at high pump powers, which indicates excellent beam mode-matching between pump and Stokes, and a high conversion efficiency. The Stokes beam profile was investigated with the increasing output power using a CMOS camera (WinCamD-LCM, DataRay Inc.) placed about 40 cm from the OC. As shown in figure 2, the beam diameter was 3.5 mm at the maximum pump power. The steady fundamental-mode Gaussian Stokes beam indicated that no thermal effects were presented in the diamond crystal at the investigated output powers.

The long-term power stability was investigated for the Stokes laser in the V-shaped and linear cavities and the pump laser for up to 15 min with a data interval of 64 ms. The RMS

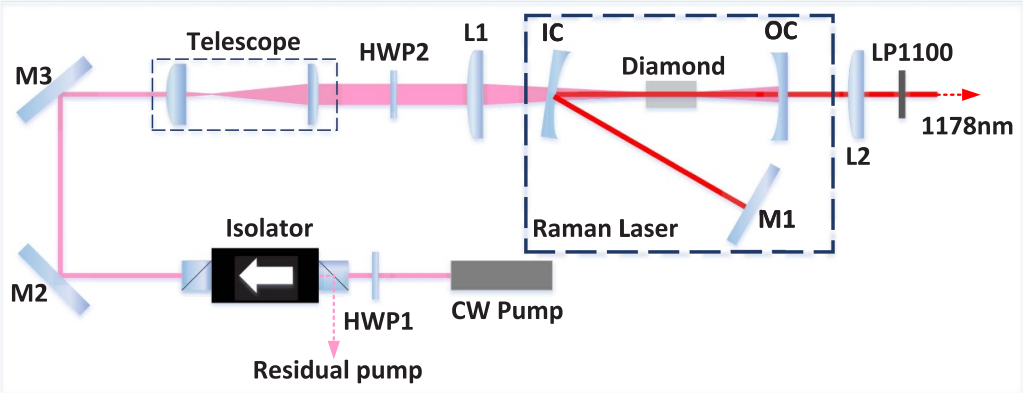

Figure 1. Experimental scheme for the external V-shaped diamond Raman cavity. HWP1/HWP2, half-wave plate (HWP); L1/L2, focusing/collimating lens; IC, input coupler; OC, output coupler; LP1100, long-pass filter @ 1100 nm.

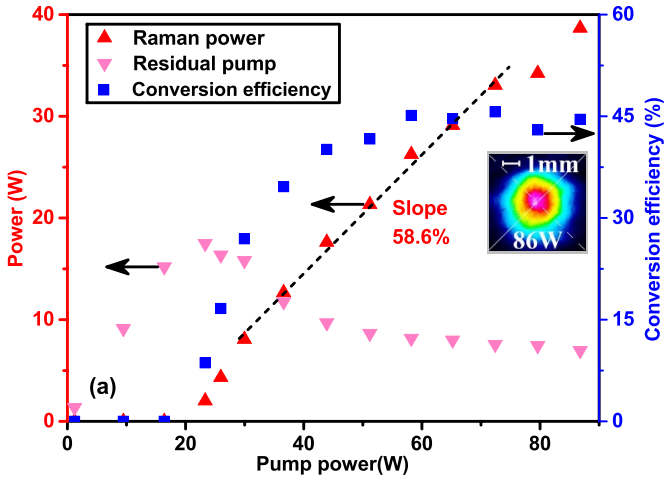

Figure 2. Measured power of Stokes (red up triangle), residual pump (pink down triangle), and conversion efficiency (blue square) in the V-shaped cavity. Inset: far-field Stokes beam profile with pump power of 86 W.

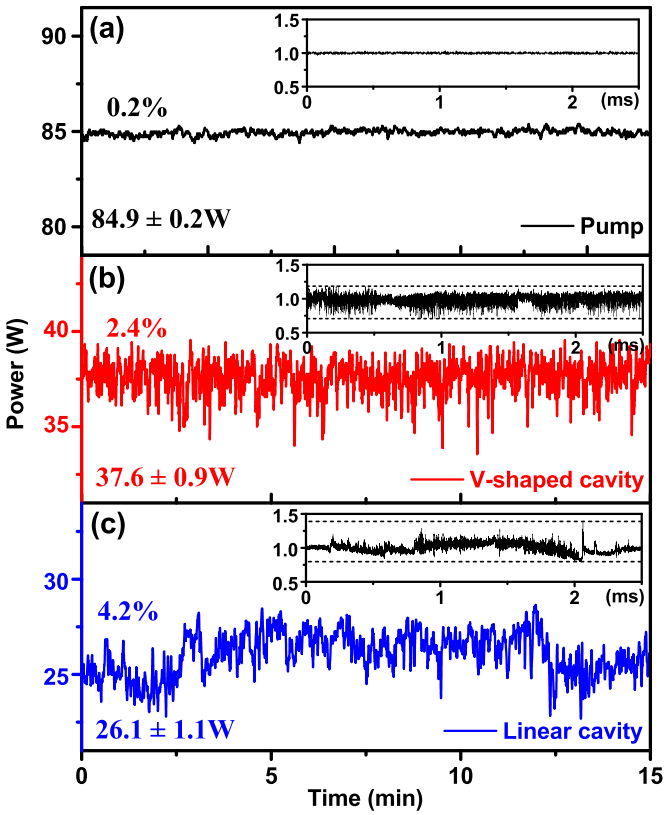

Figure 3. Long-term power stabilities of maximum output Stokes laser as well as the pump for 15 min. (a) Pump (b) V-shaped and (c) linear structured cavity. Insets: normalized temporal profiles for 2.5 ms measured by the photodiode.

of intensity fluctuations for the pump laser within 15 min was only 0.2% at 85 W, shown in figure 3(a), confirming the robustness of fiber lasers. For the V-cavity (figure 3(b)), the average power of the Stokes was 37.6 W and the RMS of the power fluctuations was 2.4%. The linear cavity delivered a Stokes output power of 26 W at the pump power of 81.6 W with the slope efficiency of 56.3%. The Stokes output-power stability in 15 min was shown in figure 3(c), where the average power was 26.1 W and the RMS of the power fluctuations was 4.2%. Fast normalized temporal profiles of the pump laser and Stokes lasers for the V-shaped and linear cavity in a 2.5 ms period were recorded using a photodiode, as shown in the insets of figure 3. The pump had almost no changes in such a short time. The short-term fluctuation of the Stokes laser was 5.7% for the V-cavity, and increased to 6.6% in the linear cavity.

Although the slope efficiencies were similar for both cavities, the V-shaped cavity had better performance in power stability, output power and conversion efficiency. First, the V-shaped cavity architecture provided a benefit over linear cavity as the introduction of M1 mirror enabled the independent adjustment of the pump beam and Stokes cavity axes resulting in a better matching of the pump and Stokes modes. Second, the V-cavity has a reduced finesse at the pump wavelength due to the double reflection on IC and the highly transmitting M1. As result, small perturbations in cavity length are less likely to affect the intracavity pump resonance and cause Stokes power instabilities [27]. The ratio of

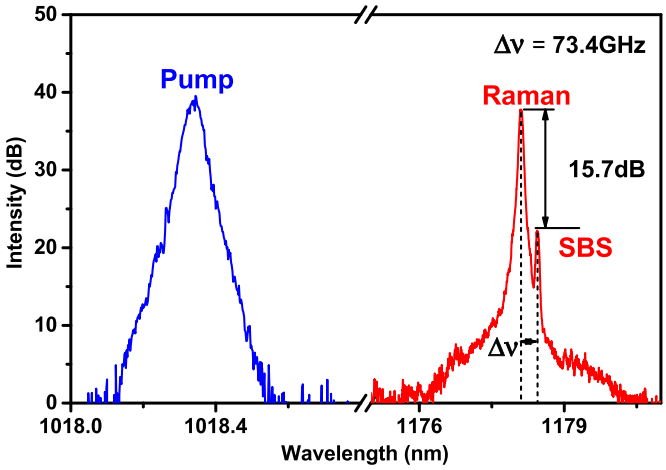

Figure 4. Typical spectra of the pump and Stokes laser at the maximum power.

the resonance to incident pump power is given by $P_{\mathrm{circ}}/P_{\mathrm{inc}} = \{(\mathrm{i}\sqrt{T_{\mathrm{IC}}})/[(1-\sqrt{R_{\mathrm{IC}}}) \times \exp(-\alpha l - \mathrm{i}\omega l/c)]\}^2$ (where α, l, ω, c are cavity loss, optical length of the cavity, resonant frequency and light speed, respectively). In the linear-cavity case, the reflectivity of IC and OC was 5.5% and 99.8%, respectively, which result in a pump resonance ratio fluctuation from 60% to 160% for a single pump longitudinal mode. The measured intracavity pump power fluctuation was 1.53%, using a sensitive photodiode (PDA20CS2, Thorlabs Inc.) for a pump power below laser threshold, which is below the calculated single-mode value due to the averaging over the pump spectrum (comprising of approximately 290 longitudinal modes spanning − 12 times wider than cavity mode spacing). In contrast, the pump resonance was negligible for the V-shaped cavity. The effective reflectivity of the IC and M1 was only 0.017% (cube of 5.5%) and so that the single mode fluctuation decreases to the range 97% to 103%. The V-shaped cavity is also less sensitive to misalignment than the linear cavity. A Jones vector analysis (reZonator software) shows with mirror displacements of 0.1°, the tilt in the cavity optical axis reduces from 0.59° to 0.25° for the V-shaped cavity.

Typical spectra for the pump and Stokes lasers in the V-shaped cavity are shown in figure 4. The center wavelength of the pump laser was 1018.3 nm with a FWHM linewidth of 12 GHz, which was fixed over the entire power range. The Stokes spectrum at the maximum output power was concentrated at the 1178.1 nm first-order Stokes line with 13.7 GHz FWHM linewidth. No coherent second-order Stokes radiation at 1397 nm was observed at this power level. However, a secondary peak at a separation 73.4 GHz appears on the longer wavelength side of the Stokes line with intensity 15.7 dB lower. The frequency shift matched the Brillouin frequency previously reported in the references of [25, 32, 40]. The emergence of SBS adversely affects the output stability and further power scaling due to the strong nonlinear coupling from the SRS field. Based on the SRS and SBS double-resonating conditions proposed in [40, 41], a solution to suppress the SBS was proposed by altering the cavity length by translating mirror M1. Using steps of 0.01 mm over a range of 12.7 mm was found not to suppress the SBS. The output Stokes power was almost unchanged during the mirror translation, indicating that no misalignment took place in the cavity. In contrast, SBS was able to be hindered in the linear structure cavity by this method. The reason is still unclear and will be further investigated in the future.

The polarization properties of the V-cavity laser were investigated as a function of incident pump polarization. The pump polarization was established with respect to the crystal [001] axis (vertical) by rotating the HWP2 and the PER of Stokes was measured using a HWP and a polarizing beamsplitting cube. As shown in figure 5, the Stokes beam was linearly polarized along the crystal [110] axis (horizontal) with a PER about 20 dB when the pump polarization over the full range of angles except from the interval 70° to 90° where the PER decreases to less than 5 dB. Note that the Stokes polarization was horizontal ellipse and vertical ellipse when the pump polarization direction and crystal [001] axis were at 90° and 80°, respectively, shown in figure 5(b). At the angle of 70°, the Stokes laser indicated a random polarization characteristic, measured with a polarimeter (PAX1000IR2/M, Thorlabs Inc.). The Stokes polarization was determined by the balance between anisotropic Raman gain and stress-induced birefringence of the diamond crystal [42]. Even though the output Stokes polarization has been analytically modeled [42], there are insufficient reports to render the experimental results related to Stokes polarizations.

This work indicates that V-cavity DRLs provide a feasible route to a stable high-power and efficient lasers at around 1.2 μm. Higher output power is expected as thermal lens effects are only expected to come into play at higher power [43]. Presently, the main challenge for power scaling is the SBS. The fact that SBS could not be suppressed with cavity length [41] indicates that mechanism for SBS generation is not well understood. The large Brillouin frequency shift of diamond crystal makes intracavity spectral filtering using volume Bragg gratings or Fabry–Pérot etalons for example, a possible method to suppress the SBS.

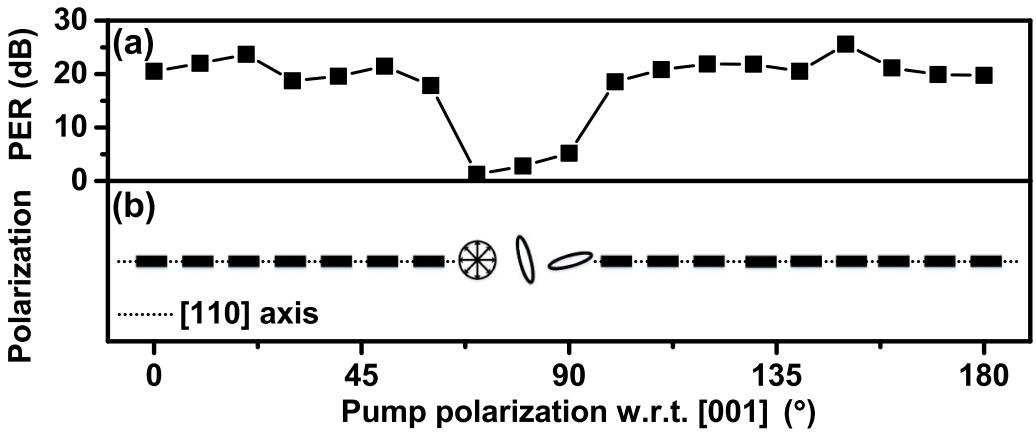

Figure 5. Polarization characteristics of Stokes laser with pump polarization angle w.r.t. the crystal [001] axis. (a) PER of the Stokes laser. (b) Polarization state of the Stokes laser w.r.t. the crystal [110] axis.

4. Conclusions

To conclude, a 39 W CW 1178 nm laser with a conversion efficiency of 45% was demonstrated in a V-shaped free-running diamond Raman resonator. The RMS of power fluctuation at maximum Stokes output was 2.4% for 15 min. The V-shaped resonator had improved conversion efficiency and stability compared with a linear standing-wave resonator. Linearly-polarized Stokes with the PER of 20 dB was achieved. These results demonstrate the prospects of folded-cavities for enabling efficient and stable high power CW output at around 1.2 μm. Notably, this work is a first step for generating a stable high-power fundamental wave at 1178 nm. In next steps, high-power and stable second harmonic generation (SHG) at 589 nm for sodium guide star is expectable by either intracavity SHG or an advanced single-frequency system that are resonantly doubled. And in the case of intracavity SHG, the Stokes spectrum is expected to be single longitudinal mode due to the nonlinear mode gain competition [33].

Acknowledgment

The authors would like to thank Chengdu Dien Photoelectric Technology Co. Ltd for the supply of the diamond crystal. This work was supported by National Natural Science Foundation of China (62005073, 61805120), National Key Research and Development Program of China (2020YFC2200300), Natural Science Foundation of Hebei Province (F2020202026) and Asian Office of Aerospace Research and Development (FA2386-21-1-403).

References

[1] Thompson L A and Gardner C S 1987 *Nature* **328** 229–31
[2] Wizinowich P L *et al* 2006 *Publ. Astron. Soc. Pac.* **118** 297
[3] Gibson A J, Thomas L and Bhattachacharyya S K 1979 *Nature* **281** 131–32
[4] Kawahara T D, Nozawa S, Saito N, Kawabata T, Tsuda T T and Wada S 2017 *Opt. Express* **25** A491–1
[5] Kane T J, Hillman P D, Denman C A, Hart M, Scott P R, Purucker M E and Potashnik S J 2018 *J. Geophys. Res.* **123** 6171–88
[6] Fan T *et al* 2019 *J. Geophys. Res.* **124** 7505–12
[7] Calvo R M, Calia D B, Barrios R, Centrone M, Giggenbach D, Lombardi G, Becker P and Zayer I 2017 *Proc. SPIE* **10096** 100960R
[8] Bennet F *et al* 2014 *Proc. SPIE* **9148** 91481F
[9] Zhang L, Jiang H, Cui S, Hu J and Feng Y 2014 *Laser Photonics Rev.* **8** 889–95
[10] Enderlein M and Kaenders W G 2016 *Opt. Photonik* **11** 31–35
[11] Yang X, Zhang L, Cui S, Fan T, Dong J and Feng Y 2017 *Opt. Lett.* **42** 4351–54
[12] Duan Y, Zhu H, Huang C, Zhang G and Wei Y 2011 Potential sodium D2 resonance radiation generated by intra-cavity SHG of a c-cut Nd:YVO4 self-Raman laser *Opt. Express* **19** 6333–8
[13] Bienfang J C, Denman C A, Grime B W, Hillman P D, Moore G T and Telle J M 2003 *Opt. Lett.* **28** 2219–21
[14] Tracy A J, Hankla A K, Lopez C, Sadighi D, Rogers N, Groff K, McKinnie I T and d'Orgeville C 2005 *OSA Technical Digest* p WA7
[15] Lu Y *et al* 2019 *Opt. Express* **27** 20282–89
[16] Sun Y, Muye L, Mildren R P, Bai Z, Zhang H, Jian L, Feng Y and Yang X 2022 High-power continuous-wave single-frequency diamond Raman laser at 1178 nm *Appl. Phys. Lett.* **121** 141104
[17] Feng Y, Huang S, Shirakawa A and Ueda K 2004 *Jpn. J. Appl. Phys.* **43** L722
[18] Liu Y, Liu Z, Cong Z, Men S, Rao H, Xia J, Zhang S and Zhang H 2016 *Opt. Laser Technol.* **81** 184–88
[19] Sheng Q, Lee A, Spence D and Pask H 2018 *Opt. Express* **26** 32145–55
[20] Chen Y F 2004 *Opt. Lett.* **29** 1251–53
[21] Wei D, Karpov V, Guo N and Clements W R L 2018 *Proc. SPIE* **10703** 107030S
[22] Men S, Liu Z, Cong Z, Liu Y, Xia J, Zhang S, Cheng W, Li Y, Tu C and Zhang X 2015 *Opt. Lett.* **40** 530–33
[23] Feng Y, Taylor L R and Calia D B 2009 *Opt. Express* **17** 23678–83
[24] Shayeganrad G 2013 *Opt. Commun.* **292** 131–34
[25] Williams R J, Nold J, Strecker M, Kitzler O, McKay A, Schreiber T and Mildren R P 2015 *Laser Photonics Rev.* **9** 405–11
[26] Williams R J *et al* 2018 *IEEE J. Sel. Top. Quantum Electron.* **24** 1–14
[27] Lux O, Sarang S, Kitzler O, Spence D J and Mildren R P 2016 *Optica* **3** 876–81

[28] Greentree A D and Prawer S 2010 *Nat. Photon.* **4** 202–3
[29] Williams R J, Kitzler O, McKay A and Mildren R P 2014 *Opt. Lett.* **39** 4152–5
[30] Feve J M, Shortoff K E, Bohn M J and Brasseur J K 2011 *Opt. Express* **19** 913–22
[31] Mildren R P and Rabeau J 2013 *Optical Engineering of Diamond* (Weinheim: Wiley-VCH)
[32] Heinzig M, Palma-Vega G, Walbaum T, Schreiber T, Eberhardt R and Tünnermann A 2020 *Opt. Lett.* **45** 2898–1
[33] Yang X, Kitzler O, Spence D J, Bai Z, Feng Y and Mildren R P 2020 *Opt. Lett.* **45** 1898–1
[34] Zhang H, Li P and Chen X 2017 *Appl. Opt.* **56** 6973–76
[35] Williams R J, Spence D J, Lux O and Mildren R P 2017 *Opt. Express* **25** 749–57
[36] Spence D J 2017 *Prog. Quantum Electron.* **51** 1–45
[37] Sabella A, Piper J A and Mildren R P 2010 *Opt. Lett.* **35** 3874–6
[38] Yang X, Bai Z, Chen D, Chen W, Feng Y and Mildren R P 2021 *Opt. Express* **29** 29449–57
[39] Bai Z, Williams R J, Jasbeer H, Sarang S, Kitzler O, Mckay A and Mildren R P 2018 *Opt. Lett.* **43** 563–66
[40] Bai Z, Williams R J, Kitzler O, Sarang S, Spence D J, Wang Y, Lu Z and Mildren R P 2020 *APL Photonics* **5** 031301
[41] Williams R J, Bai Z, Sarang S, Kitzler O, Spence D J and Mildren R P 2018 (arXiv:1807.00240)
[42] Kitzler O, Spence D J and Mildren R P 2019 *Opt. Express* **27** 17209–20
[43] Antipov S, Williams R J, Sabella A, Kitzler O, Berhane A, Spence D J and Mildren R P 2020 *Opt. Express* **28** 15232–39